20th Australasian Fluid Mechanics Conference
Perth, Australia
5-8 December 2016

Quantification of particle clusters in particle-laden round jets

N.A. Qazi[1], M. Bolla[1], H. Wang[1] and E.R. Hawkes[1,2]

[1]School of Mechanical and Manufacturing Engineering
The University of New South Wales, NSW 2052, Australia

[2]School of Photovoltaic and Renewable Energy Engineering
The University of New South Wales, NSW 2052, Australia

Abstract

In turbulent particle-laden flows, the preferential concentration of inertial particles results in multi-scale aggregates, known as 'clusters', statistical analysis of which is limited by available methods to quantify them. In this study, we analyse the data from direct numerical simulation (DNS) of a turbulent round jet, laden with particles of Stokes number (St) = 1.4. The DNS was performed in the two-way coupling regime, based on the Eulerian-Lagrangian framework and the point-particle approach, with boundary conditions consistent with the experiment (*Lau and Nathan, J. Fluid Mech. 2014, 757, 432-457*). A novel method, which is a combination of statistical box-counting, thresholding and image-processing, is used to identify and characterise the clusters from a two-dimensional thin layer at the center of the jet. A quasi-quantitative comparison with the experimental results reveals that the DNS is able to predict the trends observed in the experiment. The results further show that the characteristic dimensions of the clusters follow a log-normal distribution. On a logarithmic scale, the PDF (probability distribution functions) of the cluster area are found to follow a power-law distribution with an exponent equal to -2. It is further confirmed that the clusters exhibit a complex fractal nature in DNS as well as the experiment.

Introduction

Turbulent particle-laden jet flows find applications in various industrial and engineering processes such as pulverised coal combustion, industrial sprays and solar thermochemical systems. In turbulent particle-laden flows, the inability of inertial particles to follow the local flow streamlines results in accumulation of particles, creating large inhomogeneities in the particle concentration field [3, 11]. This phenomenon is commonly referred to as "preferential concentration" or "clustering". There is experimental evidence that the instantaneous preferential concentration of particles in such systems significantly impacts their performance, affecting heat transfer, stoichiometry and emissions [15]. Consequently, accurate prediction of particle distributions in particle-laden turbulent jet flows is crucial, considering their effects on the evaporation and combustion processes followed.

Since the early 1990s, the advancement in technology for simulations as well as experiments has advanced our understanding of particle clusters (see [11] for review on the subject). The general consensus is that the clustering is maximum for Stokes number (based on the Kolmogorov length scale), St, approaching unity and monotonically decreases (increases) with the Stokes number when $St > 1$ ($St < 1$). However, a number of issues still persist, especially regarding the quantification of these regions of highly dense and/or depleted particle concentrations [1, 11]. A thorough statistical characterization of the particle clusters is imperative both to the development of a detailed understanding of the particle dispersion process and to the validation of models of particle dispersion in turbulent flows.

In order to quantitatively estimate the characteristic dimensions of the clusters, two basic steps are involved. Firstly, the clusters need to be identified. The "box counting method", where the particle concentration is calculated by digitising the domain by boxes of equal size and counting the number of particles in each box [1] in conjunction with a suitable threshold [4] are usually employed. Once clusters are identified, a further step is required to measure and classify the characteristic dimensions of these clusters. The accuracy of the available methods, such as "equivalent ellipse" [13] and "bent-object algorithm" [5], deteriorates for larger structures with multiple branches, particularly the under- and over-estimation of the length and the width of the structures. As a consequence, neither of these methods is suitable for use on clusters with highly irregular, wrinkled, or branched shapes. In contrast, a morphological skeletonization method [6], in conjunction with a pruning algorithm [2], proposed in [9] has been demonstrated to estimate the characteristic dimension of the particle clusters with an uncertainty of ~3% of the manually determined values.

In this paper, we demonstrate a methodology which can be directly applied to datasets obtained from numerical simulations to gain insights into the characteristic dimensions of the particle clusters. The data was generated in our previous work [14] through DNS of particle-laden round jet. Four DNS cases of different Stokes number (St = 0.3, 1.4, 5.6 and 11.2), based on the Eulerian-Lagrangian framework and point-particle approach, were performed in the two-way coupling regime. In the present work, only the results from St = 1.4 are discussed. The Stokes number of order unity is selected due to its particular relevance in the study of industrial burners and solar thermo-chemical reactors [8]. The particle clusters are locally identified and characterised by employing thresholding techniques and the skeletonisation method [9]. The results are compared with the available experimental results [9]. In particular, we present the first computations of the characteristic dimensions of particle clusters from DNS of a two-phase turbulent round jet.

Methodology

DNS of particle-laden round jet

The simulation setup has been detailed in a previous work [14], and only a brief description is provided here. Figure 1 presents the schematics of the computational domain for the particle-laden round jet configuration. The computational domain extends to $L_x \times L_y \times L_z = 30D \times 25D \times 25D$ in the streamwise and the two lateral directions, respectively. In the simulations, special attention has been given to ensure that the inlet conditions for the jet, including the mean axial flow velocity, mean axial particle velocity and the concentration distribution of the particles at the jet exit, match well with those measured in the experiment [8]. In the experiment, a continuous number of clusters have been detected from the nozzle exit which arises from the pipe flow. This effect could not be included in the DNS as the spatio-temporal correlate-

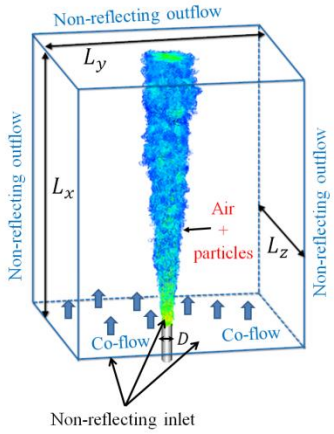

Figure 1. A schematic of the particle-laden round jet configuration.

ions of particle concentration have not been accounted for, i.e. the DNS doesn't inject clustered structures at the nozzle exit. This simplification may result in certain disagreement between the results, especially close to the nozzle exit. Further information on the simulation setup, computational method and related results can be found elsewhere [14].

Identification of Particle Clusters

The step-by-step methodology of cluster identification is presented in figure 2. It is started from the instantaneous scatter of the Lagrangian particles positions on the two-dimensional (2D) thin layer (thickness $0.04D$) of the jet as shown in figure 2a. The slice thickness $0.04D$ is approximately same as the one of the laser sheet employed in the experiment ($\approx 0.0276D$), to ensure that the sampling volume is consistent. In a first step, the corresponding instantaneous particle concentration map C_i (figure 2b) is obtained using the box counting method with a box size of $L_B = 0.08D$.

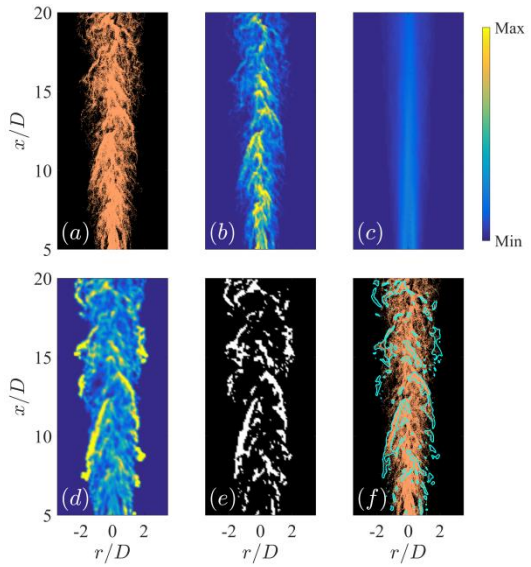

Figure 2. Stages of identification of particle clusters from the DNS for box size, $L_B = 0.08D$. A part of the domain is shown for clarity.

A three-dimensional (3D) circular Gaussian spatial filter, similar to that in [4], is then applied to smoothen C_i. From the instantaneous snapshots, a mean concentration map C_m (figure 2c) is obtained by averaging C_i over the available dataset. Subsequently, in figure 2d the instantaneous smoothed concentration maps are normalised by the mean, viz. $\overline{C_i} = C_i/C_m$. The clusters are then defined as the connected regions with a normalized concentration higher than a threshold value C_{th}. Here, based on a sensitivity analysis (not shown here for brevity), $C_{th} = 1.70$ has been used to discern the clusters and to generate the binary image (figure 2e) drawing the clusters in white. Finally, for visualization, the boundaries of the clusters are extracted and superimposed on the instantaneous snapshot of particles, shown in figure 2f.

Characterisation of Particle Clusters: Skeletonisation

The skeletonisation method has been discussed in detail previously [9] and only a brief description is included here with the visual support of figure 3. Upon identification of a cluster from the binary image described above in figure 2e, a pruned morphological skeleton is generated which consists of a series of lines (branches) equidistant from the boundary of the original image. The length of the cluster L_c is approximated by the length of the longest segment of the pruned skeleton. Figure 3a presents a typical cluster boundary along with the corresponding pruned skeleton.

The characteristic width of the cluster W_c was calculated based on a two-step procedure. Firstly, a first-pass estimate of the width was obtained by taking the average of $2d_{min,i}$, where $d_{min,i}$ is the distance between each point i on the skeleton and its nearest boundary. Next, each skeleton branch was then shortened by half this amount to produce a trimmed skeleton, as shown in figure 3b. The characteristic cluster width W_c is then the average of $2d_{\mathrm{min,j}}$, where j is now each point on the trimmed pruned skeleton. From the calculated width, an inverse skeleton was produced for each image by applying a constant width of W_c to the trimmed, pruned skeleton as shown in figure 3b. From the values of the cluster length and width, the cluster aspect ratio is calculated as $AR_c = L_c/W_c$.

The perimeter of a cluster is estimated by calculating the distance between each adjoining pair of pixels around the border of the inverse skeleton. Similarly, the area of the cluster is the number of the pixels in the region marked by the inverse skeleton. The exact same methodology is then applied to the experimental dataset to compute the area and the perimeter of the 2D cluster slices.

The above methodology is applied to the central 2D slice of the jet from the DNS to a full dataset of ≈ 422 different time instants, homogeneously distributed across 7 jet flow-through times. In the present work, only the clusters of area $A_c > 0.04D^2$ were selected for analysis. The elimination of the small features (clusters) that are not attached to the main features was performed with the use of a morphological operator 'image opening' [13].

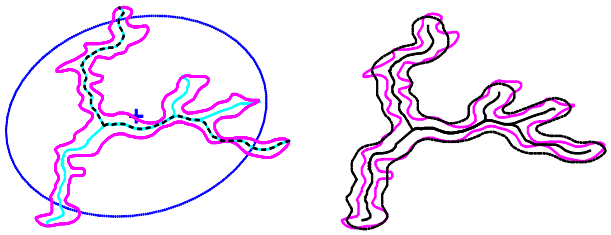

(a) *(b)*

Figure 3. Characterisation of particle clusters through the skeletonisation method. (*a*) Estimation of length of clusters through length of the longest segment of the pruned skeleton, (– – –) boundary of the identified cluster, (– – –) pruned skeleton, (– – –) longest segment, (– – –) equivalent ellipse, (+) Centroid; (*b*) Boundary of inverse skeleton superimposed on original cluster boundary, (– – –) Boundary of the identified cluster, (– – –) trimmed pruned skeleton, (– . –) inverse skeleton.

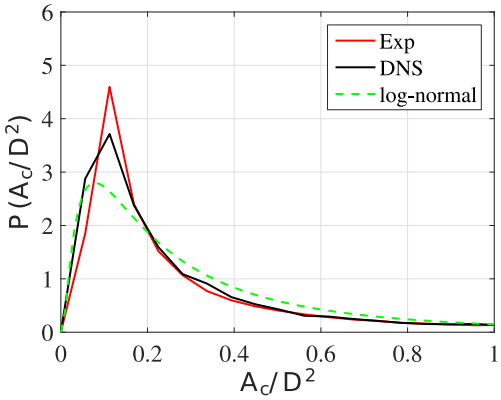

Figure 4. The comparison of PDF of the cluster areas for the experiment and DNS. A log-normal distribution is generated analytically for the mean and standard deviation of the DNS dataset.

Results and Discussion

Geometrical Properties of Particle Clusters

A comparison of the PDF of cluster area from the experiment and the DNS is presented in figure 4. The figure shows that the behaviour of the PDFs is qualitatively similar for both the experimental and the numerical dataset and provides confidence that the DNS is able to reproduce the trends observed in the experiment. It is noted that the PDF is analogous to a log-normal distribution (red dashed line). Similar results have been previously observed in other investigations of particle-laden flows as well [11] and the log-normal distributions have been observed for the thickness of the scalar dissipation structures (layers) [16] and thermal gradient structures in a non-premixed flame [7] as well. Currently, there is no complete theoretical interpretation of this log-normality, but these results indicate a potential for future modeling efforts.

Figure 5 shows the same data as in figure 4, but on a log-log scale. The figure shows that except for very small areas, the PDF follows a power law with an exponent approximately equal to -2. Interestingly, this behaviour has been previously observed in particle laden flows in isotropic turbulence, independent of the simulation/experiment and of the particle Stokes number [11]. These results indicate the important (and possibly universal) self-similar characteristics of the preferential accumulation of particles at the small scales. Further investigations are required to confirm this hypothesis.

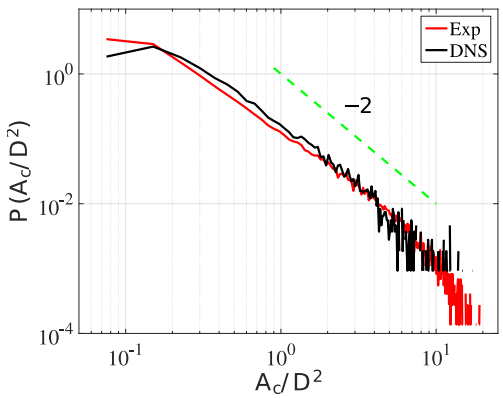

Figure 5. The comparison of PDF of cluster area on a log-log scale.

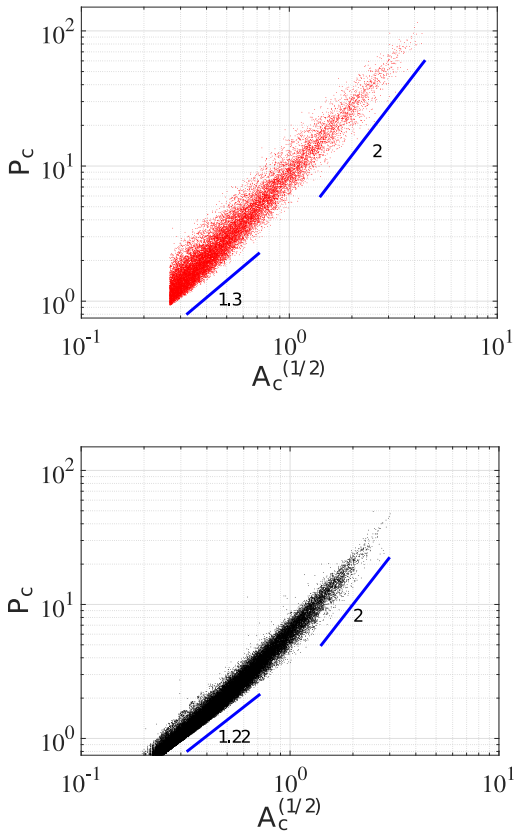

Figure 6. The relation between cluster area and perimeter. (top) experiment; (bottom) DNS.

Fractal Nature of Particle Clusters

Prior works regarding the cluster shapes in isotropic turbulence have evidenced that the individual particle clusters exhibit fractal structures [11], and hence are self-similar. The fractal dimension (d) of an object can be computed through the perimeter-area relationship [10] viz. $p = k.A^{(d/2)}$, where p is the perimeter and A is the area. For a certain geometrical object, $d \approx 1$ represents a smooth and compact surface (e.g. for a circle, $d = 1$). Conversely, $d \gtrsim 2$ represents a highly fractal, branched structure. Figure 6 shows the relation of the perimeter (P_c) and the square root of the area of the identified clusters from the experiment (top) and the DNS (bottom). The results show that the small, compact structures $(\sqrt{A_c} \lesssim 0.7)$ are approximately linearly related (representing a smooth, circular structure), whereas the larger clusters $(\sqrt{A_c} \gtrsim 2)$ exhibit a complex fractal structure. There features have been found to be always present for particle clusters (also for the depleted regions, known as 'holes') [1, 11, 12], irrespective of the simulation/experimental configuration. The fractal dimensions of the particle clusters from some selected previous works are included in Table 1. The values of the fractal dimension of the compact structures are close in all the cases. Similarly, the fractal dimensions of the larger structures is found in the range $1.6 \leq d \leq 2$.

Cluster geometry	DNS	Exp, Ref. [8]	Ref. [1]	Ref. [12]
Compact	1.22	1.3	1	1.2
Fractal	2	2	1.6	1.7

Table 1. A comparison of the fractal dimension of the clusters between the current datasets and previous results.

Conclusion

A quantitative assessment of preferential concentration has been performed in turbulent particle-laden round jet configuration. A novel method which is a combination of statistical box-counting, thresholding and image-processing has been demonstrated to accurately estimate the local characteristic dimensions of the particle clusters for the St = 1.4 particles. A quasi-quantitative comparison is performed with the corresponding experiment and the results show that the simulation is able to reproduce the trends observed in the experiments to a reasonable degree of accuracy. The results further show that the cluster areas follow log-normal distributions for both experimental and the numerical dataset. On a log-log scale, the PDF of cluster area is found to follow a power law with exponent ≈ -2, similar to other works for isotropic turbulence. The fractal nature of the particle clusters is confirmed in the present case of shear-driven flow.

Acknowledgments

This research was carried out with the funding support from Australian Renewable Energy Agency (ARENA) and Australian Research Council (ARC). The research was performed using computational resources sponsored by the Department of Energy's Office of Energy Efficiency and Renewable Energy, located at the National Renewable Energy Laboratory (NREL). R. Grout acknowledges the support of the Department of Energy Office of Advanced Scientific Computing Research. The research also benefited from the Australian Research Council and the computational resources provided through the National Computational Merit Allocation Scheme, supported by the Australian Government. The computational facilities supporting this project included the Australian NCI National Facility, the partner share of the NCI facility provided by Intersect Australia Pty Ltd., the Peak Computing Facility of the Victorian Life Sciences Computation Initiative (VLSCI), iVEC (Western Australia), and the UNSW Faculty of Engineering.

References

[1] Aliseda, A., et al., Effect of preferential concentration on the settling velocity of heavy particles in homogeneous isotropic turbulence. *Journal of Fluid Mechanics*, 2002. **468**: p. 77-105.

[2] Bai, X., L.J. Latecki, and W.-Y. Liu, Skeleton pruning by contour partitioning with discrete curve evolution. *Pattern Analysis and Machine Intelligence, IEEE Transactions on*, 2007. **29**(3): p. 449-462.

[3] Balachandar, S. and J.K. Eaton, Turbulent Dispersed Multiphase Flow. *Annual Review of Fluid Mechanics*, 2010. **42**(1): p. 111-133.

[4] Birzer, C.H., P.A.M. Kalt, and G.J. Nathan, A method to provide statistical measures of large-scale instantaneous particle clusters from planar images. *Experiments in Fluids*, 2011. **51**(3): p. 641-656.

[5] Chan, Q.N., P.R. Medwell, and G.J. Nathan, Algorithm for soot sheet quantification in a piloted turbulent jet non-premixed natural gas flame. *Experiments in Fluids*, 2014. **55**(10).

[6] Jahne, B. and B. Jaehne, *Practical handbook on image processing for scientific applications*. 1995: CRC Press, Inc.

[7] Kaiser, S.A. and J.H. Frank, Imaging of dissipative structures in the near field of a turbulent non-premixed jet flame. *Proceedings of the Combustion Institute*, 2007. **31**(1): p. 1515-1523.

[8] Lau, T.C.W. and G.J. Nathan, Influence of Stokes number on the velocity and concentration distributions in particle-laden jets. *Journal of Fluid Mechanics*, 2014. **757**: p. 432-457.

[9] Lau, T.C.W. and G.J. Nathan, A method for identifying and characterising particle clusters in a two-phase turbulent jet. *Experiments in Fluids (under review)*, 2015.

[10] Mandelbrot, B.B., *The fractal geometry of nature*. Vol. 173. 1983: Macmillan.

[11] Monchaux, R., M. Bourgoin, and A. Cartellier, Analyzing preferential concentration and clustering of inertial particles in turbulence. *International Journal of Multiphase Flow*, 2012. **40**: p. 1-18.

[12] Monchaux, R., M. Bourgoin, and A. Cartellier, Preferential concentration of heavy particles: A Voronoï analysis. *Physics of Fluids*, 2010. **22**(10): p. 103304.

[13] Qamar, N.H., et al., Soot sheet dimensions in turbulent nonpremixed flames. *Combustion and Flame*, 2011. **158**(12): p. 2458-2464.

[14] Qazi, N.A., et al., *Direct numerical simulation of the influence of Stokes number on velocity and particle concentration distributions in particle-laden round jets*, in *8th International Symposium on Turbulence, Heat and Mass Transfer (THMT'15)*. 2015: E306, Sarajevo, Bosnia and Herzegovina.

[15] Smith, N., et al., The significance of particle clustering in pulverized coal flames. *Proceedings of the Combustion Institute*, 2002. **29**(1): p. 797-804.

[16] Su, L.K. and N.T. Clemens, The structure of fine-scale scalar mixing in gas-phase planar turbulent jets. *Journal of Fluid Mechanics*, 2003. **488**: p. 1-29.